Check for updates

| Bacteriology | Research Article

In silico and *in vitro* comparative analysis of 79 *Acinetobacter baumannii* clinical isolates

Martina Scarrone,[1,2] Dann Turner,[3] Moïra Dion,[1] Denise Tremblay,[1,2,4] Sylvain Moineau[1,2,4]

AUTHOR AFFILIATIONS See affiliation list on p. 12.

ABSTRACT *Acinetobacter baumannii* is a significant nosocomial bacterial pathogen that poses a substantial infection risk due to its high resistance to antibiotics and ability to survive in hospital environments. In this study, we performed comprehensive *in silico* and *in vitro* analyses on 79 *A. baumannii* clinical isolates from different geographical locations to uncover their genomic and epidemiological characteristics as well as their antibiotic and phage susceptibilities. Our findings revealed considerable genomic diversity among the isolates, as shown by average nucleotide identity (ANI) heat maps, multilocus sequence typing (MLST), and core genome MLST (cgMLST). We identified several international clones known for their high antibiotic resistance and global prevalence. Surprisingly, we also observed that the number of antimicrobial resistance genes (ARGs) was higher in isolates containing CRISPR-Cas systems. Plaque assays with 13 phages indicated that *Acinetobacter* phages have a narrow host range, with capsule loci (KL) serving as a good indicator of phage-bacteria interactions. The presence of CRISPR-Cas systems and other antiviral defense mechanisms in *A. baumannii* genomes also appears to play a key role in providing phage resistance, regardless of the phage receptors. We also found that spacers associated with subtypes I-F1 and I-F2 CRISPR-Cas systems predominantly target prophages, suggesting a role in maintaining genomic stability and contributing to phage-bacteria co-evolution. Overall, this study provides a set of highly characterized *A. baumannii* clinical isolates for future studies on antibiotic-phage-bacteria interactions.

IMPORTANCE *Acinetobacter baumannii* poses a significant challenge to the healthcare system due to its antibiotic resistance and strong survival mechanisms. This study examines a diverse collection of 79 clinical isolates to deepen our understanding of *A. baumannii*'s genetic characteristics and its defense mechanisms against both antibiotics and phages. Genomic analysis revealed globally prevalent, highly resistant clones and uncovered a complex role for CRISPR-Cas systems. Although CRISPR-Cas systems were not widespread among these isolates, they primarily targeted prophages. Additionally, the study emphasizes the importance of capsule types as indicators of phage susceptibility. Together, these findings provide insights into the pathogen's resilience and evolutionary adaptations, potentially guiding future research on infection control strategies and new therapeutic approaches to combat *A. baumannii* infections.

KEYWORDS *Acinetobacter baumannii*, antimicrobial resistance (AMR), bacteriophages, phages, CRISPR-Cas, capsule loci (KL), multilocus sequence typing (MLST)

*A*cinetobacter baumannii is an opportunistic bacterial pathogen known to cause fatal nosocomial infections worldwide (1). It has been ranked as a critical priority for the development of therapeutics by the World Health Organization due to its intrinsic high resistance to several antibiotics and its ability to rapidly acquire resistance to those in clinical use (2–4). *A. baumannii* is commonly detected and isolated from hospital

environments and intensive care units, causing infections such as bacteremia, ventilator-associated pneumonia, endocarditis, meningitis, urinary tract infections, and wound infections (5), though environmental and animal reservoirs have also been identified (6, 7).

A wide range of virulence factors contribute to the pathogenesis and elevated mortality associated with *A. baumannii* infections, including outer membrane proteins, lipopolysaccharides, capsular polysaccharides (CPS), iron-acquisition systems, efflux pumps, and biofilm production (8, 9). These virulence factors allow the evasion of the immune system and play a role in the survival of the pathogen and its antimicrobial resistance (AMR) (8, 10). The cell-surface CPS is one of the key determinants in *A. baumannii* as it plays a central role in its ability to cause disease, evade host defenses, and persist in hospital environments. Highly diverse CPS structures have been observed due to the polymorphism of the capsule loci (KL), accounting for at least 237 KI identified so far in *A. baumannii* (11–13). CPS typing is also of interest because it represents a target for therapies, including antibody-based approaches or bacteriophages (phage therapy) (13, 14).

Multilocus sequence typing (MLST) is another powerful strain characterization tool that has allowed the population and epidemiology studies of a variety of pathogens, including *A. baumannii* (15). However, this approach has limitations as a phylogeny inferred from MLST fails to represent the true genomic relationships within the same bacterial species (16, 17). Core genome MLST (cgMLST) is a more extensive tool that encompasses a larger set of gene loci (hundreds to thousands instead of six to seven for MLST), enabling high-resolution bacterial genotyping (18).

A few studies have started to address the associations between the various capsule and sequence types along with the presence of carbapenem resistance genes (19–22). This information could be key for tracking the spread of this pathogen. Yet, little is known about the relationship between these features and whether there are additional underlying relationships with AMR. For example, the presence of defense systems, such as CRISPR-Cas systems, which target bacteriophages and plasmids, could restrict AMR acquisition through horizontal gene transfer (23). So far, two CRISPR-Cas systems (subtypes I-F1 and I-F2) have been predominantly identified in *A. baumannii*, though their prevalence was estimated at only 14% among nearly 5,000 isolates (24). This underscores the need to explore other defense systems as well.

Here, we performed comprehensive *in silico* and *in vitro* analyses of 79 clinical isolates of *A. baumannii*. We examined genomic diversity, KL typing, sequence types (STs), antibiotic resistance profiles, phage resistance, and antiviral defense systems. Our findings revealed significant genomic variation and key international clones linked to high antibiotic resistance. We explored the complexity of phage susceptibility, where KL typing serves as a useful predictor of phage infection, albeit it is likely influenced by various antiviral defense systems. Additionally, we found that CRISPR spacers in our set of *A. baumannii* isolates predominantly target prophages, suggesting a role in genomic stability and evolution. These insights underscore the potential for targeted therapeutic strategies, including phage therapy and novel approaches to disrupt CPS structures.

MATERIALS AND METHODS

Bacterial isolates, phages, and media

A total of 79 *A. baumannii* clinical isolates were obtained from various sources worldwide, and they are listed in Table S1. They were cultured with agitation at 37°C in Luria-Bertani broth (LB) (Fisher, Tryptone 10 g/L, yeast extract 5 g/L, sodium chloride 10 g/L). Thirteen *A. baumannii* phages were also used in this study, and their conditions of propagation are described in Table S2. Biological materials were stored at −80°C with 15% (vol/vol) glycerol.

Bacterial genomic DNA extraction, sequencing, and assembly

Bacterial genomic DNA was extracted from the 79 *A. baumannii* isolates following a phenol-chloroform protocol (25). Illumina DNA Prep kit and Integrated DNA Technologies 10 bp unique dual indexes were used for library preparation prior to genome sequencing. Paired-end reads (2 × 151 bp) were generated with an Illumina NovaSeq 6000 sequencer (SeqCenter, Pittsburgh, PA, USA). Demultiplexing, quality control, and adapter trimming were performed with bcl-convert1 (v4.1.5). Assembly was performed with both Spades v3.13.0 (26) and Ray v3.0.1-rc (27), and the assemblies with the best coverage were kept. Genome completeness and contamination levels were calculated using CheckM2 (28).

Genome similarity analyses

Average nucleotide identity (ANI) was calculated using FastANI with default settings (K-mer size = 16, fragment length = 3,000). The ANI results were visualized as a hierarchically clustered heatmap using the scipy and seaborn libraries in Python. For the cgMLST analysis, the *A. baumannii* schema that uses 2,390 loci (version 30/05/2021 [29]) was downloaded from www.cgMLST.org and adapted for use with chewBBACA (30), using the PrepExternalSchema module. The cgMLST clustering analysis was performed using ReporTree v2.5.4, implementing the MSTreeV2 method from GrapeTree v1.5.0, with clusters of closely related isolates being determined at ≤9 allelic differences (31). The minimum spanning tree was constructed and visualized using GrapeTree v1.5.0 (32). A maximum likelihood phylogenetic tree was inferred using IQTree2 version 2.3.4 (33) with the best fit model predicted by ModelFinder (34) using the concatenated MAFFT alignment of the set of 577 core loci from the chewBBACA analysis. Branch supports were obtained using 1000 Ultra-fast bootstrap (35) and SH-Alrt test replicates. The tree was visualized and annotated with metadata using iTOL (36).

Multilocus sequence typing and capsular polysaccharide typing

The public database for molecular typing (PubMLST) web software (37) was used to determine the MLST profile and ST of the 79 isolates using the whole genome sequencing(WGS) assemblies and according to the Pasteur scheme (38). Whenever the results did not show a 100% identity for each allele to determine the ST accurately, a PCR was performed (38), followed by Sanger sequencing to confirm the allele. CPS typing was performed with Kaptive v. 2.0.0 using the updated *A. baumannii* KL reference sequence database (13), which was downloaded from https://github.com/katholt/Kaptive (accessed in December 2023). The KL was assigned to an isolate if the match confidence was predicted as good or higher.

Antimicrobial susceptibility *in vitro* and antibiotic-resistance genes *in silico*

Susceptibility of the 79 isolates to 17 clinically approved antibiotics was tested *in vitro* by disk diffusion or minimal inhibitory concentration (MIC) test following the guidelines recommended by the Clinical and Laboratory Standards Institute (CLSI) (39) with 16 commercial antimicrobial disks of ceftazidime, imipenem, doripenem, tetracycline, ciprofloxacin, sulfamethoxazole/trimethoprim, piperacillin (Hardy Diagnostics, Santa Maria, CA, USA), ampicillin-sulbactam, cefepime, cefotaxime, meropenem, tobramycin, gentamicin, amikacin, minocycline, and levofloxacin (BD, Quebec City, QC, Canada). The 17th antibiotic, colistin sulfate (Sigma-Aldrich, St. Louis, MO, USA), was tested with the MIC test. Quality controls were performed for every antibiotic with *Escherichia coli* ATCC 25922. Genes mediating antimicrobial resistance from *A. baumannii* draft genomes were identified with the web server ResFinder v 4.5.0 using default thresholds of ≥80% coverage and ≥60% identity (40).

Transmission electron microscopy

Phage morphology was confirmed or identified by transmission electron microscopy (TEM) as previously described (41) and using phosphotungstic acid-stained phage preparations.

Phage host range determination

For the *in vitro* phage sensitivity assay, the 79 bacterial isolates were challenged with the lysates ($>10^6$ PFU/mL) of 13 phages using standard spot test assays ($n = 2$) (42). Briefly, a top layer of LB with 0.75% (wt/vol) agar (supplemented with 10 mM $CaCl_2$ when needed) inoculated with 100 µL of bacterial overnight culture was added to plates containing a bottom layer of LB with 1.5% (wt/vol) agar. A 5 µL volume of serial 10-fold phage dilutions (50 mM Tris-HCl, pH 7.5, 100 mM NaCl, and 8 mM $MgSO_4$) was spotted onto the bacterial overlay, and the plates were incubated at 37°C overnight. A bacterial isolate was considered susceptible to a phage when the lysis zone was observed at least at dilution 10^{-2}. As controls, phages were spotted onto their propagating hosts.

Phage defense systems

Analysis on the antiviral defense systems of the 79 bacterial isolates was performed on their genome sequences using the software PADLOC v2.0.0 with models v2.0.0 (43). Candidate defense systems that have not been validated experimentally in other bacterial species were excluded from the results.

CRISPR-Cas systems predictions and CRISPR array analysis

Identification of CRISPR-Cas systems and their arrays was performed with the web versions of both CRISPRCasFinder (44, 45) and CRISPRDetect (46) (accessed in February 2024) with default parameters. Both outputs were manually compared and curated to meet the cut-off criteria for a predicted valid array: 28 bp long direct repeats (DR) with at least 85% identity within the same array, and evidence level 4 or higher in CRISPRCas-Finder. A colony PCR was also performed to confirm the presence of separate CRISPR arrays using the following specific primers: 5′-GGATTTCCTGCAATGACGGC-3′ (forward) and 5′-TCTAAAGCATCACGCCCCTG-3′ (reverse) for I-F1 and 5′-CCTGATCTTGTGCTTGGCGA -3′(forward) and 5′-GTGGTGCCGTGTTTATTGGT-3′ (reverse) for I-F2. CRISPRStudio (47) was used to produce a color-coded figure of the CRISPR arrays with default parameters, using as inputs the curated CRISPRDetect GFF format outputs. Spacer analyses were conducted in a Jupyter notebook using the Python 3.10.6 packages pandas and matplotlib.pyplot. Three databases were queried for the presence of spacer targets (protospacers) using blastn v 2.12.0 (48): the NCBI Virus database (filtered for Virus; bacteriophage, downloaded on 15 April 2024), the plasmid database PLSDB v 2023_11_03_v2 (49, 50) (downloaded on 15 April 2024), and a comprehensive database of 2,055 prophage sequences from 450 *A. baumannii* complete genomes (D. Turner, unpublished data). A protospacer was considered a target when the alignment showed at most four mismatches on the full length of the spacer and zero gaps. For correlation analyses, violin plots were generated using the aforementioned Python 3.10.6 packages, and Mann-Whitney U from scipy.stats and seaborn.

RESULTS AND DISCUSSION

Genomic data, phylogeny, MLST, and cgMLST of 79 *A. baumannii* isolates

A total of 79 *A. baumannii* isolates were obtained from institutes around the world, with the aim of generating a diverse collection. Genomic DNA extraction, sequencing, and assembly were performed for all isolates. Confirmation of the bacterial species was done by identification of the *bla-OXA-51-like* gene, which is intrinsic to *A. baumannii* (51). The average coverage for the draft genomes was 43.7X ± 12.4, and the average GC content was 39.0% ± 0.1 %. An ANI heat map was created to facilitate the genomic comparison of the bacterial isolates and to identify relationships (Fig. 1). The heatmap

FIG 1 Genomic comparison of 79 *A. baumannii* isolates. Heat map of the average nucleotide identity (ANI). ANI values were determined using FastANI, and the heatmap was hierarchically clustered using the complete linkage method. Clonal complexes CC1, CC2, and CC15 are indicated on the left. *, isolate that does not belong to CC1.

revealed significant clustering among the isolates, indicating a high degree of genomic similarity between certain groups. As an example, the upper left cluster shows six isolates (CCRI 19670, CCRI 19671, CCRI 19672, CCRI 19674, CCRI 19675, and CCRI 19677) with ANI values ≥99.9% (dark red in Fig. 1), which suggests that they are highly related. A similar clustering was observed with other isolates as well (e.g., CCRI 14160, CCRI 14161, CCRI 14162, CCRI 14163, CCRI 14164, CCRI 14165, and CCRI 14166). Conversely, the heatmap also highlighted genomic diversity among other isolates, as evidenced by overall ANI

values ranging between 97.3% and 99.9 %. These more distant evolutionary relationships among these bacterial isolates (52) are likely explained by the different sources and geographical locations they were isolated (Table S1).

To further study the genetic relationships among the 79 bacterial isolates, a minimum spanning tree (MST) was created for the cgMLST (Fig. 2), which allows for high-resolution genotyping. An ST was assigned to each isolate according to their MLST profile (Pasteur scheme), and they were subsequently grouped into a given clonal complex (CC), both informative of the population structure, distribution, and epidemiology (53). We observed a great diversity in terms of the phylogenetic lineages. Twenty-eight STs were identified, with ST1 (11/79) and ST2 (13/79) being the two most predominant. ST1 and ST2 are known to belong to the CC1 and CC2, respectively, two globally distributed lineages comprising carbapenem-resistant strains of high risk (38, 54, 55). The CC1 included ST1 and ST81 (also represented in the first upper left cluster square in Fig. 1). When we explored the geographical origin of the isolates (Table S1), we observed that all ST81 isolates, originating from Canada, were highly related (Fig. 1). For ST1, most isolates came from Europe, including Belgium (1), the Czech Republic (1), France (2), and the Netherlands (4), while others were isolated in North America (Canada, 1) and South America (Argentina, 1), with one isolate of unknown origin. A similar pattern was observed for CC2 (the second upper left cluster square in Fig. 1), composed of ST2 and ST47 isolates. Most ST2 isolates originated from Europe, including the Czech Republic (2), Georgia (1), Germany (2), Italy (1), the Netherlands (2), Spain (1), and the United Kingdom (1). One isolate was from North America (Canada), and two had no geographical information. The single ST47 isolate originated from the Czech Republic. Lastly, CC15, which includes isolates from ST15 and ST238, comprised five ST15 isolates from Argentina and one ST238 isolate from Canada. CC15 has previously been reported as a successful clonal complex in South America (56, 57).

A maximum likelihood phylogenetic tree was also created to study the evolutionary relationships and ancestral lineages among the isolates and to compare it to their STs (Fig. 3A). Expectedly, bacterial isolates clustered in a similar pattern as shown in the ANI heat map and the MST tree for cgMLST (Fig. 1 and 2). However, we could observe the differences in evolutionary history among isolates belonging to the same ST. This was particularly evident for ST2, where the main ancestral branch encompassing all ST2 isolates splits into two distinct groups, highlighting differences in their evolutionary trajectories.

In silico and in vitro relationship between ST and AMR

The association between the ST and AMR profiles of the isolates can provide a better understanding of the population structure and epidemiology of this pathogen (58). We assessed the antimicrobial resistance in vitro against 17 clinically approved antibiotics for human use (Fig. 3B; Table S1). The antibiotics that proved to be most effective were ampicillin-sulbactam and minocycline, successful against 70/79 and 62/79 isolates, respectively. On the other hand, isolates were more resistant to piperacillin and sulfamethoxazole/trimethoprim, as 21/79 and 25/79 were sensitive to these antibiotics. These results agree with some of the previous reports on A. baumannii clinical isolates (29, 59, 60).

We observed widely diverse resistance profiles (average of 7.0 ± 5.0 resistances per isolate). Eleven isolates were sensitive to all the antibiotics, while others showed resistance to all antibiotics of a specific class, with one isolate being resistant to all 17 antibiotics under our laboratory conditions (ANC 5190, ST2). Specific STs were resistant to more antibiotics, notably ST1, ST2, ST15, ST78, ST84, and ST91. This is in line with previous studies, where CC1 (which comprises ST1, ST84, and ST91 in this study), CC2 (ST2), and ST15 also showed multidrug resistance (29). ST2 is well recognized as a major cause of outbreaks and is associated with higher disease severity and mortality (61).

We also predicted the number of AMR genes (ARGs) in each assembled genome (Fig. 3B; Table S3). The average number of ARGs per isolate was 5.0 ± 2.7, with the
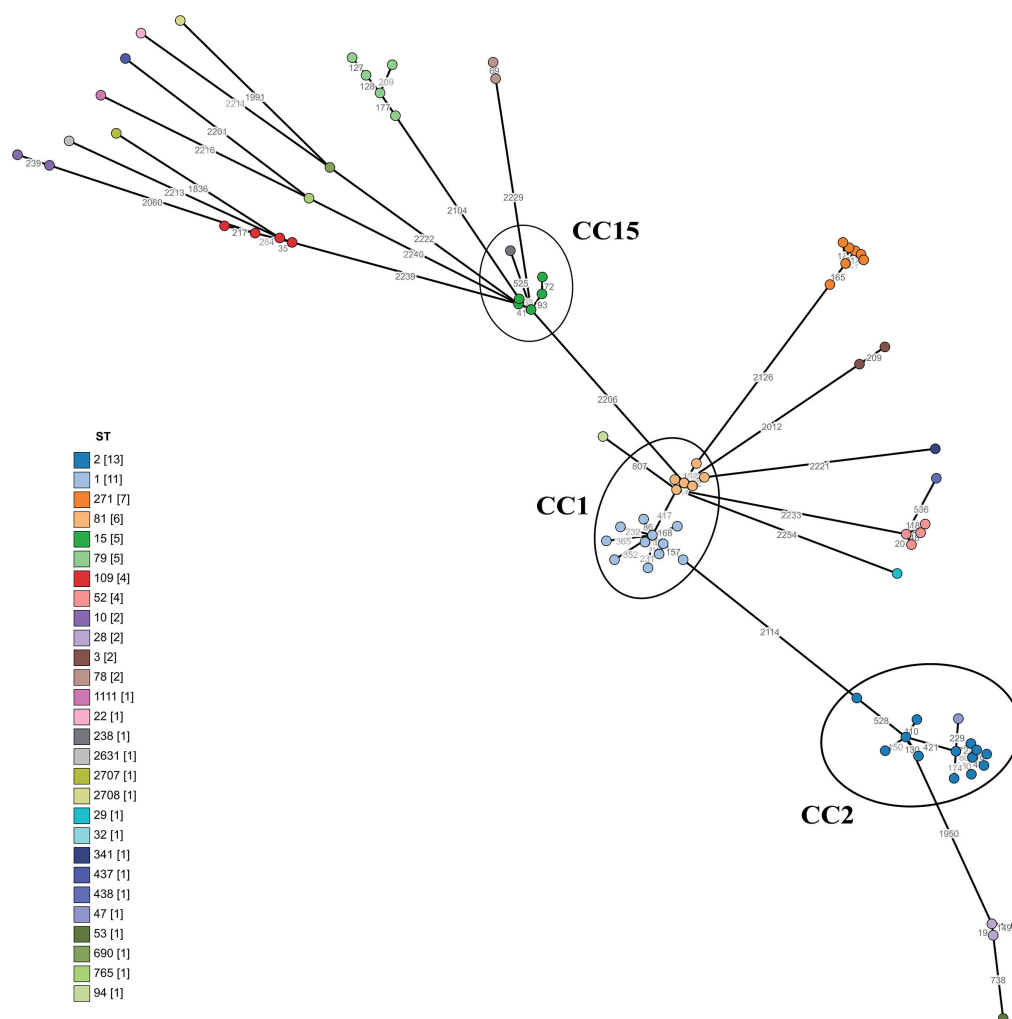
FIG 2 Minimum spanning tree analysis of 79 *A. baumannii* isolates. Representation of the genetic relationships among the cgMLST profiles of the 79 *A. baumannii* isolates. Each circle (node) in the tree corresponds to an individual cgMLST profile, colored according to the sequence type (ST, Pasteur scheme) as indicated in the legend, with the number of isolates shown in brackets. The edges connecting the nodes indicate genetic distances between profiles, with shorter edges representing smaller genetic differences. The numbers on the edges denote the number of allelic differences out of 2,390 alleles. CC1, CC2, and CC15 are circled, each comprising STs that share a single allelic mismatch according to the MLST Pasteur scheme (seven alleles).

cephalosporinase-encoding gene *blaADC-25* being present in 78/79 isolates. Only the isolate NCTC 13302 did not carry that gene. This analysis only comprised the acquired ARGs and does not consider possible mutations that may have a direct or indirect impact on AMR. In some cases, the number of AMR *in silico* and *in vitro* seemed to correlate well (the more AMR *in vitro*, the more ARGs), but no significant statistical correlation was observed when all isolates were compared (Pearson coefficient: −0.16). Of note, the *in silico* analysis also included genes conferring resistance to antibiotics that are not clinically approved for human use (as per the CLSI guidelines) and were therefore not tested *in vitro*.

Capsule loci, phage host range, and antiviral defense systems

The CPS is one of the main virulence factors in *A. baumannii* and frequently serves as a receptor to initiate phage infection (62–64). The KL, which contains the genomic information to produce the CPS, was predicted with good to perfect confidence for most
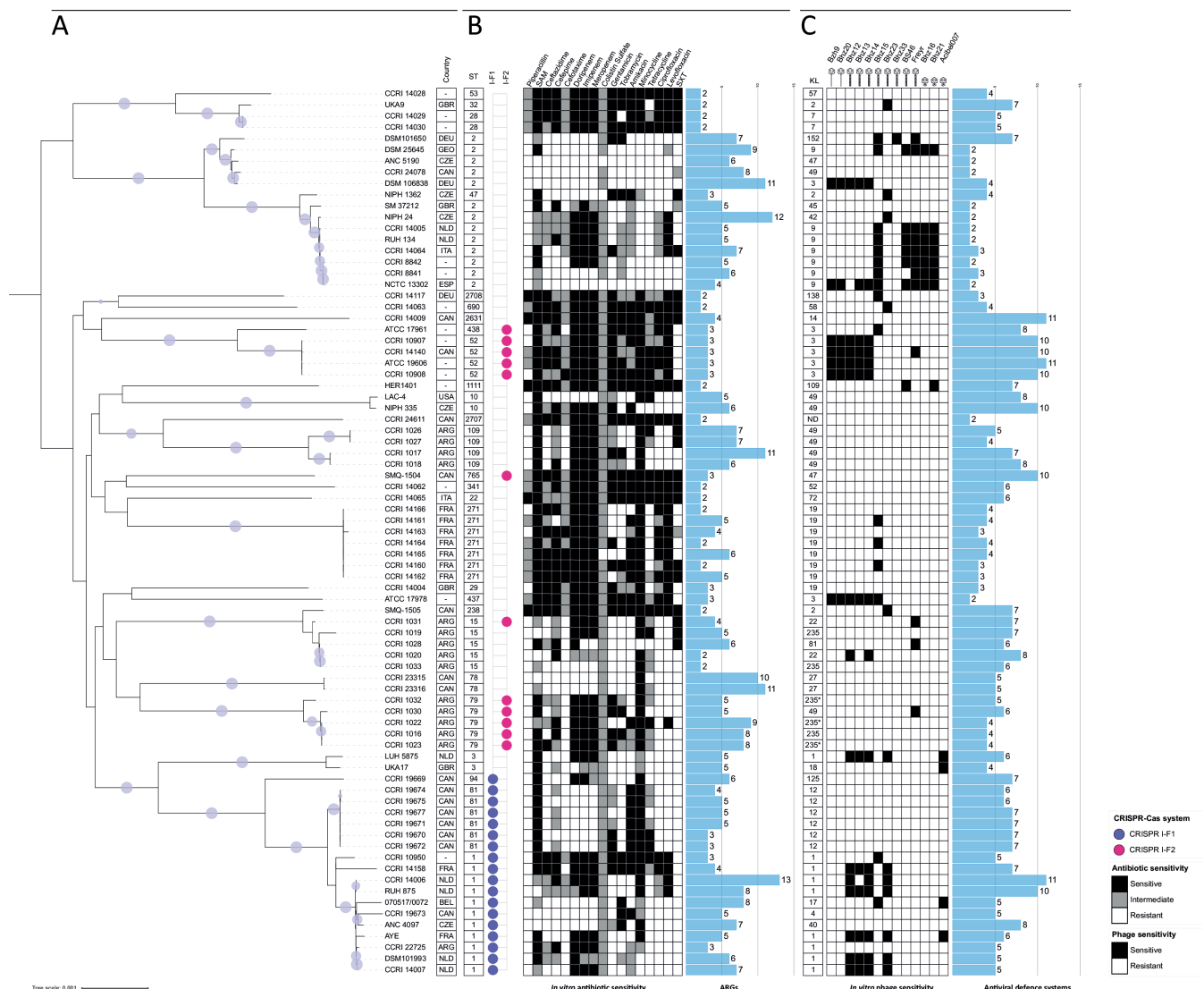
FIG 3 Comparative analysis of 79 *A. baumannii* isolates. (A) The maximum likelihood phylogenetic tree was inferred from the concatenated alignment of a set of 577 core loci. The tree is rooted at the midpoint, and ultra-fast bootstrap support ≥95% is shown as filled circles. The country of origin of each *A. baumannii* isolate, when available, is shown adjacent to the leaf labels as a three-letter country code: ARG (Argentina), BEL (Belgium), CAN (Canada), CZE (Czech Republic), DEU (Germany), ESP (Spain), FRA (France), GBR (United Kingdom), GEO (Georgia), ITA (Italy), NLD (Netherlands), and USA (United States). Additionally, the designated ST and the presence of subtype I-F1 (purple dot) or subtype I-F2 (fuchsia dot) CRISPR-Cas systems are indicated. (B) Susceptibility of the *A. baumannii* isolates to 17 antibiotics is shown as a heat map, colored according to the key on the right side of the figure. The bar chart denotes the predicted number of antimicrobial resistance genes (ARGs) from the *in silico* analysis. (C) The designated KL for each *A. baumannii* isolate is shown, as well as the sensitivity to 13 phages as a heat map, colored according to the key also on the right. The bar charts denote the predicted number of phage defense systems from the *in silico* analysis. *, low confidence of prediction; ND, not determined.

of the isolates (75/79, Fig. 3C). Three isolates (CCRI 1022, CCRI 1023, and CCRI 1032) had a low confidence prediction, which is likely attributed to draft genome assemblies. One isolate (CCRI 24611) showed no confidence of prediction, which may indicate the presence of a new KL not reported in the database. In total, there were 28 different KL (and one not determined), with KL1 being the most predominant (nine isolates), followed by KL49 (8), KL19 (8), KL3 (7), and KL9 (7). The different KLs did not cluster according to the phylogeny as did the STs (Fig. 3A). Thus, isolates belonging to the same KL can belong to different lineages.

The 79 *A. baumannii* isolates were challenged with 13 phages representing three morphotypes (Fig. 3C): two siphoviruses (long non-contractile tails), eight myoviruses

(long contractile tails), and three podoviruses (short non-contractile tails). These phages, along with their bacterial hosts, were sourced from various laboratories across the globe to ensure the inclusion of the three most common *Caudoviricetes* morphotypes in our set of phages. Virion morphologies were confirmed by TEM (Fig. S1), and further information on these phages, their original hosts, and propagation conditions can be found in Table S2. Most *A. baumannii* isolates were resistant to all or most phages, and thus, these *A. baumannii* phages have a narrow host range. Each phage infected between 1 and 16 isolates, with phage Bhz33 having the smallest host range (1) and Bhz15 the broadest (16). In total, the set of phages infected 39 *A. baumannii* isolates. Generally, the phage host range correlated well with the KL typing, regardless of phage morphology. Several phages were capable of infecting more than one KL, usually ranging from 1 to 4 KL. Interestingly, two myophages, Freyr and Bhz15, were able to infect six and seven KL types, respectively, although this infection capability did not extend to all isolates within each KL type.

Since the CPS can be required to initiate a successful phage infection, KL may represent a key predictor of host recognition. However, the presence of intracellular defense systems could still block the phage infection process and affect the host range, even when there is phage adsorption (65). Using *in silico* analyses, the average number of defense systems per isolate was estimated at 5.5 ± 2.5 (Fig. 3C). Fifty-one systems were identified across the isolates, most of which were found in only one or a few (Table S4). The DMS_other and Mokosh type II antiviral defense systems appeared in 38 and 37 isolates, respectively. However, the PADLOC category DMS_other includes antiphage systems that may be incomplete and may not represent a distinct system. Of note, we found no statistical significance between the *in vitro* phage resistance and the *in silico* number of defense systems (Pearson coefficient: 0.059).

When comparing antiviral defense systems among the isolates within the same KL group, there was a difference in the number of systems per isolate. Taking the seven isolates of the KL3 group as an example, the antiviral defense systems ranged from 2 to 11 per isolate. Interestingly, we observed that one KL3 isolate (ATCC 17961) was sensitive to only one phage instead of five phages for the others. When we compared the type of antiviral defense systems (Table S4), ATCC 17961 was predicted to have six antiviral defense systems in common with other isolates of the same KL, as well as two unique ones: PD-Lambda-2 and cbass_type_II (66, 67). The presence of these additional systems may explain the difference observed in phage susceptibility.

Taken altogether, these findings suggest that predicting the success of the phage-bacteria interaction in *A. baumannii* will require a more comprehensive analysis. However, the association between KL type and phage specificity represents a good start.

Presence of CRISPR-Cas systems in *A. baumannii*

A total of 29 of the 79 *A. baumannii* isolates (36.7%, Fig. 3A; Table S5) were found to possess a CRISPR-Cas system based on CRISPRCasFinder and CRISPRDetect tools. Two subtypes were represented (68): I-F1 (in 18 isolates) and I-F2 (in 11 isolates), which correlates with previous findings, in which the prevalence of the I-F1 subtype was higher in *A. baumannii* (24, 69). Their presence and subtyping were also confirmed by detecting the genes *csy2* (I-F1) and *cas7f2* (I-F2) by PCR. Notably, two separate CRISPR arrays were detected in five isolates that contained the I-F2 subtype.

We identified an association between certain STs and the presence of CRISPR-Cas systems I-F1 and I-F2 (Fig. 3A), as previously reported (24). The subtype I-F1 was observed in all ST1 and ST81 isolates (CC1) and in the only ST94 isolate, which is closely related to ST1 and ST81 in terms of phylogeny and genomic similarity (Fig. 1 and 2). As for the subtype I-F2, it was observed in all isolates assigned to ST79 and ST52. Subtype I-F2 was also seen in the only ST438 (belonging to CC52 along with the ST52) and ST765 isolates.

CRISPR spacers predominantly target *A. baumannii* prophages

A total of 1,753 spacers, of which 338 were unique, were identified in the 34 CRISPR arrays of the 29 *A.* isolates. The average number of spacers per array was 51.6 ± 18.1. This number was higher for the arrays of the I-F1 systems compared to the I-F2 (60.2 ± 19.6 and 41.8 ± 9.9, respectively). The highest and lowest number of spacers were 84 and 18, respectively, with both arrays belonging to the I-F1 system. The spacer length was almost exclusively 32 bp, whereas the DRs were always 28 bp. The consensus DR sequences had 67.9% pairwise identity between the two subtypes: 5′-GTTCATGGCGG CATACGCCATTTAGAAA-3′ (I-F1) and 5′-GTTCTTCATCGCATAGATGATTTAGAAA-3′ (I-F2). A schematic representation of the spacers is illustrated in Fig. 4, and spacer information is found in Table S5. A high spacer homology was found within the same subtype, with a few exceptions, reflected by the number of arrays sharing the same diamond–square color combination (Fig. 4). Those isolates with identical CRISPR arrays (see CCRI19670, CCRI19672, CCRI19674, CCRI19675, CCRI19677) also had very high ANI (Fig. 1).

All spacers were blasted against three databases: the NCBI Virus database filtered for bacteriophages (42,648 nucleotide results and 168 RefSeq genomes), the PLSDB database for plasmids (50,554 sequences), and a prophage database (2,055 prophage sequences from 450 *A. baumannii* isolates), representing a total of 95,245 sequences. Of the 1,753 spacers, 889 (50.7%) had a matching sequence in at least one of the databases and against 1,646 different targets. The targeting spacers were distributed across the arrays, with no tendency to accumulate closer to the 5′ or 3′ end (Fig. S2), which indicates that they likely represent both recent and historical acquisitions, respectively (70). The number of matching sequences per spacer varied significantly, with spacers having only one target and others with over 500 targets, which can be attributed to the overrepresented conserved genes within prophage sequences. The spacers targeted 21 phages (1.3% of the 1,646 targets), which were either virulent, temperate, or filamentous, 133 plasmids (8.1%), and 1,492 *A. baumannii* prophages (90.6%). Of the 21 phages, 15 (71%) corresponded to *A. baumannii* phages. From the remaining targeted phages, they were from human gut metagenomes, one *Inoviridae* from an animal metagenome, and an *Erwinia* phage. Out of the 133 targeted plasmids, 129 (97%) were from *Acinetobacter* species, including among others *baumannii* (70), *seifertii* (13), *nosocomialis* (10), *pittii* (7), *indicus* (5), and *bereziniae* (4). Three different species from the *Edwardsiella* genus and one from *Agrobacterium* were also found, all Gram-negative bacteria. These results aligned with previous findings for *A. baumannii* CRISPR arrays in which, out of the spacers with identified matching sequences, a majority targeted temperate phages (24).
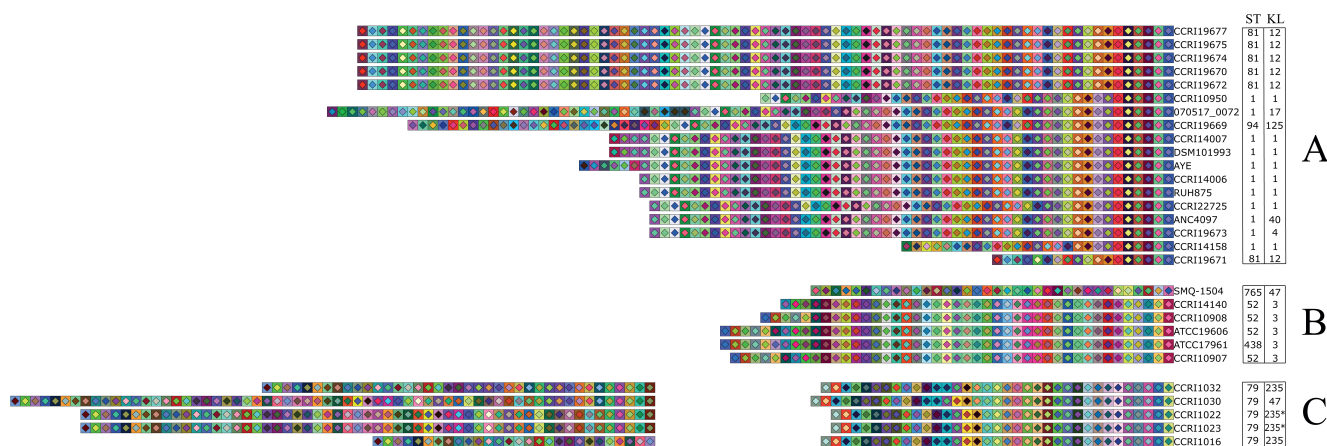
FIG 4 Schematic representation of spacers from CRISPR arrays in *A. baumannii* isolates. Each colored square corresponds to a spacer, ordered from 5′ to 3′ end. Two spacers with the same diamond–square color combination share homologous sequences. The designated ST and KL for each *A. baumannii* isolate are shown adjacent to their arrays. "*": Low confidence in prediction. Isolates were grouped by CRISPR-Cas subtype: (A) I-F1, (B) I-F2, and (C) I-F2 containing two CRISPR arrays.
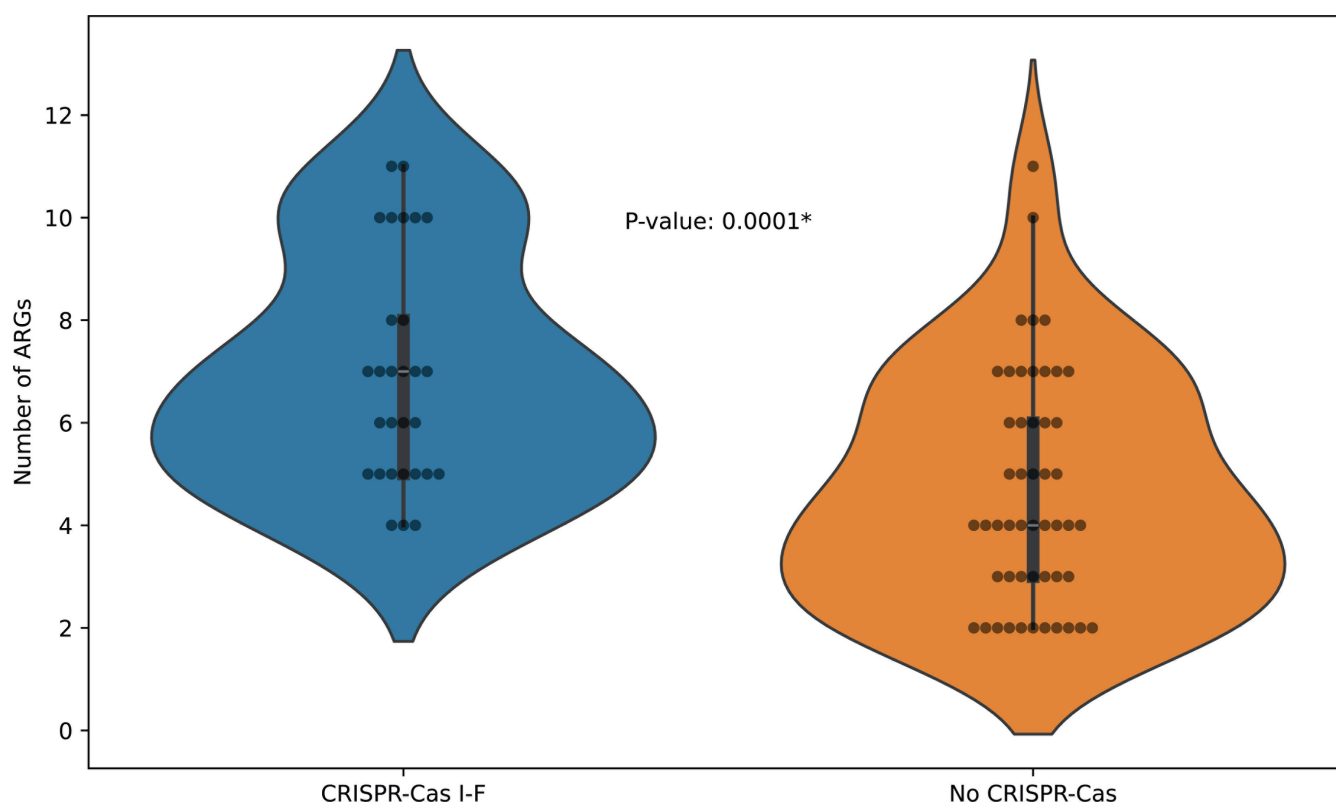
FIG 5 Distribution of ARGs in *A. baumannii* isolates with or without a subtype I-F CRISPR-Cas system. Violin plot depicting the number of ARGs in isolates with the presence of the subtype I-F CRISPR-Cas system (blue) and without any CRISPR-Cas system (orange). Mann-Whitney U test was performed to determine the *P*-value of 0.0001 (significant *P*-value < 0.05).

Relationships between ARGs and CRISPR-Cas arrays

We compared our set of *A. baumannii* isolates in terms of the presence and absence of CRISPR-Cas systems with AMR and phage susceptibility (both *in vitro* and *in silico*). No significant correlation was found for most associations analyzed, except for the number of ARGs (Fig. 5). The distribution of ARGs shifted to a higher number of ARGs per isolate for those containing a CRISPR-Cas system (either I-F1 or I-F2), compared to the isolates lacking one. This is in contradiction with previous reports for this bacterial pathogen and others, as strains containing CRISPR-Cas systems tend to carry fewer antibiotic resistance genes (69, 71, 72). Others also observed that isolates carrying CRISPR-Cas systems lacked plasmids (73, 74), which supports the protective function of the CRISPR-Cas system against foreign invading DNA, like plasmids, and the acquisition of ARGs through mobile genetic elements (75–77). On the other hand, a previous *in silico* analysis reported that *A. baumannii* isolates carrying the subtype I-F CRISPR-Cas system had no association with resistance or virulence genes, with just a few exceptions. While no spacers were found to directly target these genes, they instead targeted plasmids (24). Yet, in another study, the presence of CRISPR-Cas systems did not correlate with the presence of ARGs in 104,947 reference genomes (from 5,677 bacterial species) (78). This would suggest that the CRISPR-Cas system would not hinder the dissemination of these genes, unless specifically plasmid-borne (78). In this study, we did not find any spacer targeting ARGs in plasmids according to the PLSDB metadata.

Collectively, this underlines that the mechanisms of action and regulation of CRISPR-Cas systems in relation to the acquisition of ARGs through mobile genetic elements are complex, and there are probably other factors like anti-CRISPR proteins or endogenous gene regulation yet to be defined (79). Moreover, while this CRISPR-AMR

correlation was evidenced *in silico*, no significant correlation was found between the AMRs *in vitro*.

Conclusion

In summary, this work has resulted in the creation of a well-characterized library of 79 clinical isolates of *A. baumannii*. The comprehensive *in vitro* and *in silico* analyses of these isolates enhance our understanding of this pathogen. The findings highlight the prevalence of certain international clones, though the factors contributing to their success need further investigation. Phage susceptibility in *A. baumannii* appears complex, with the KL serving as a good indicator of phage-bacteria interactions. Yet, the presence of CRISPR-Cas and other antiviral defense systems underscores their potential impact on these interactions. Moreover, we found that the CRISPR-Cas systems predominantly target prophages as observed by others (80, 81), potentially defending against latent threats if prophages enter the lytic cycle, promoting genomic stability, or contributing to the phage-bacteria coevolution. Future research should explore the diversity of isolates beyond clinical samples to gain a more comprehensive understanding of the population structure of *A. baumannii*. A more detailed characterization of bacterial and phage receptors, molecular mechanisms of lytic infection, as well as a deeper exploration of the defense mechanisms, will be needed for phage therapy to be successful against this critically important bacterial pathogen. Ultimately, these approaches will contribute to the development of novel therapeutic strategies against *A. baumannii* infections.

AUTHOR AFFILIATIONS

[1]Département de biochimie, de microbiologie et de bio-Informatique, Faculté des sciences et de génie, Université Laval, Quebec City, Quebec, Canada
[2]Institut de biologie intégrative et des systèmes (IBIS), Université Laval, Quebec City, Quebec, Canada
[3]School of Applied Sciences, College of Health, Science and Society, , University of the West of England, Bristol, United Kingdom
[4]Félix d'Hérelle Reference Center for Bacterial Viruses, Université Laval, Quebec City, Quebec, Canada

AUTHOR ORCIDs

Martina Scarrone http://orcid.org/0000-0003-4300-2818
Denise Tremblay http://orcid.org/0009-0008-7544-1739
Sylvain Moineau http://orcid.org/0000-0002-2832-5101

AUTHOR CONTRIBUTIONS

Martina Scarrone, Conceptualization, Data curation, Formal analysis, Investigation, Methodology, Resources, Validation, Visualization, Writing – original draft, Writing – review and editing, Software | Dann Turner, Formal analysis, Investigation, Methodology, Software, Validation, Visualization, Writing – review and editing | Moïra Dion, Data curation, Formal analysis, Methodology, Software, Validation, Visualization, Writing – review and editing | Denise Tremblay, Data curation, Methodology, Resources, Writing – review and editing | Sylvain Moineau, Conceptualization, Data curation, Formal analysis, Funding acquisition, Investigation, Methodology, Project administration, Resources, Supervision, Validation, Visualization, Writing – review and editing

DATA AVAILABILITY

Assembled draft whole genome sequences were submitted to the National Center for Biotechnology Information (NCBI) as BioProject PRJNA1081428. Accession numbers for each BioSample can be found in Table S1. Bacterial genomes were annotated during the NCBI submission using the Genome Annotation Pipeline (PGAP). Additional information is available on request from the corresponding author.

ADDITIONAL FILES

The following material is available online.

Supplemental Material

Supplemental figures (Spectrum02849-24-s0001.docx). Fig. S1 and S2.
Supplemental tables (Spectrum02849-24-s0002.xlsx). Tables S1 to S8.

REFERENCES

1. Mohd Sazlly Lim S, Zainal Abidin A, Liew SM, Roberts JA, Sime FB. 2019. The global prevalence of multidrug-resistance among *Acinetobacter baumannii* causing hospital-acquired and ventilator-associated pneumonia and its associated mortality: a systematic review and meta-analysis. J Infect 79:593–600. https://doi.org/10.1016/j.jinf.2019.09.012

2. Peleg AY, Seifert H, Paterson DL. 2008. *Acinetobacter baumannii*: emergence of a successful pathogen. Clin Microbiol Rev 21:538–582. https://doi.org/10.1128/CMR.00058-07

3. Tacconelli E, Carrara E, Savoldi A, Harbarth S, Mendelson M, Monnet DL, Pulcini C, Kahlmeter G, Kluytmans J, Carmeli Y, Ouellette M, Outterson K, Patel J, Cavaleri M, Cox EM, Houchens CR, Grayson ML, Hansen P, Singh N, Theuretzbacher U, Magrini N, WHO Pathogens Priority List Working Group. 2018. Discovery, research, and development of new antibiotics: the WHO priority list of antibiotic-resistant bacteria and tuberculosis. Lancet Infect Dis 18:318–327. https://doi.org/10.1016/S1473-3099(17)30753-3

4. Havenga B, Ndlovu T, Clements T, Reyneke B, Waso M, Khan W. 2019. Exploring the antimicrobial resistance profiles of WHO critical priority list bacterial strains. BMC Microbiol 19:303. https://doi.org/10.1186/s12866-019-1687-0

5. Son H-J, Cho EB, Bae M, Lee SC, Sung H, Kim M-N, Jung J, Kim MJ, Kim S-H, Lee S-O, Choi S-H, Woo JH, Kim YS, Chong YP. 2020. Clinical and microbiological analysis of risk factors for mortality in patients with carbapenem-resistant *Acinetobacter baumannii* bacteremia. Open Forum Infect Dis 7:ofaa378. https://doi.org/10.1093/ofid/ofaa378

6. Eveillard M, Kempf M, Belmonte O, Pailhoriès H, Joly-Guillou ML. 2013. Reservoirs of *Acinetobacter baumannii* outside the hospital and potential involvement in emerging human community-acquired infections. Int J Infect Dis 17:e802–5. https://doi.org/10.1016/j.ijid.2013.03.021

7. Maravić A, Skočibušić M, Fredotović Ž, Šamanić I, Cvjetan S, Knezović M, Puizina J. 2016. Urban riverine environment is a source of multidrug-resistant and ESBL-producing clinically important *Acinetobacter* spp. Environ Sci Pollut Res 23:3525–3535. https://doi.org/10.1007/s11356-015-5586-0

8. Dehbanipour R, Ghalavand Z. 2022. *Acinetobacter baumannii*: pathogenesis, virulence factors, novel therapeutic options and mechanisms of resistance to antimicrobial agents with emphasis on tigecycline. J Clin Pharm Ther 47:1875–1884. https://doi.org/10.1111/jcpt.13787

9. Shadan A, Pathak A, Ma Y, Pathania R, Singh RP. 2023. Deciphering the virulence factors, regulation, and immune response to *Acinetobacter baumannii* infection. Front Cell Infect Microbiol 13:1053968. https://doi.org/10.3389/fcimb.2023.1053968

10. Wong D, Nielsen TB, Bonomo RA, Pantapalangkoor P, Luna B, Spellberg B. 2017. Clinical and pathophysiological overview of *Acinetobacter* infections: a century of challenges. Clin Microbiol Rev 30:409–447. https://doi.org/10.1128/CMR.00058-16

11. Talyansky Y, Nielsen TB, Yan J, Carlino-Macdonald U, Di Venanzio G, Chakravorty S, Ulhaq A, Feldman MF, Russo TA, Vinogradov E, Luna B, Wright MS, Adams MD, Spellberg B. 2021. Capsule carbohydrate structure determines virulence in *Acinetobacter baumannii*. PLoS Pathog 17:e1009291. https://doi.org/10.1371/journal.ppat.1009291

12. Kenyon JJ, Hall RM. 2013. Variation in the complex carbohydrate biosynthesis loci of *Acinetobacter baumannii* genomes. PLoS One 8:e62160. https://doi.org/10.1371/journal.pone.0062160

13. Cahill SM, Hall RM, Kenyon JJ. 2022. An update to the database for *Acinetobacter baumannii* capsular polysaccharide locus typing extends the extensive and diverse repertoire of genes found at and outside the K locus. Microb Genom 8. https://doi.org/10.1099/mgen.0.000878

14. Singh JK, Adams FG, Brown MH. 2018. Diversity and function of capsular polysaccharide in *Acinetobacter baumannii*. Front Microbiol 9:3301. https://doi.org/10.3389/fmicb.2018.03301

15. Maiden MC, Bygraves JA, Feil E, Morelli G, Russell JE, Urwin R, Zhang Q, Zhou J, Zurth K, Caugant DA, Feavers IM, Achtman M, Spratt BG. 1998. Multilocus sequence typing: a portable approach to the identification of clones within populations of pathogenic microorganisms. Proc Natl Acad Sci USA 95:3140–3145. https://doi.org/10.1073/pnas.95.6.3140

16. Tsang AKL, Lee HH, Yiu SM, Lau SKP, Woo PCY. 2017. Failure of phylogeny inferred from multilocus sequence typing to represent bacterial phylogeny. Sci Rep 7:4536. https://doi.org/10.1038/s41598-017-04707-4

17. Castillo-Ramírez S, Graña-Miraglia L. 2019. Inaccurate multilocus sequence typing of *Acinetobacter baumannii*. Emerg Infect Dis 25:186–187. https://doi.org/10.3201/eid2501.180374

18. Uelze L, Grützke J, Borowiak M, Hammerl JA, Juraschek K, Deneke C, Tausch SH, Malorny B. 2020. Typing methods based on whole genome sequencing data. One Health Outlook 2:3. https://doi.org/10.1186/s42522-020-0010-1

19. Wyres KL, Cahill SM, Holt KE, Hall RM, Kenyon JJ. 2020. Identification of *Acinetobacter baumannii* loci for capsular polysaccharide (KL) and lipooligosaccharide outer core (OCL) synthesis in genome assemblies using curated reference databases compatible with Kaptive. Microb Genom 6. https://doi.org/10.1099/mgen.0.000339

20. Luo YC, Hsieh YC, Wu JW, Quyen TLT, Chen YY, Liao WC, Li SW, Wang SH, Pan YJ. 2022. Exploring the association between capsular types, sequence types, and carbapenemase genes in *Acinetobacter baumannii*. Int J Antimicrob Agents 59:106470. https://doi.org/10.1016/j.ijantimicag.2021.106470

21. Hsieh YC, Wang SH, Chen YY, Lin TL, Shie SS, Huang CT, Lee CH, Chen YC, Quyen TLT, Pan YJ. 2020. Association of capsular types with carbapenem resistance, disease severity, and mortality in *Acinetobacter baumannii*. Emerg Microbes Infect 9:2094–2104. https://doi.org/10.1080/22221751.2020.1822757

22. Koncz M, Stirling T, Hadj Mehdi H, Méhi O, Eszenyi B, Asbóth A, Apjok G, Tóth Á, Orosz L, Vásárhelyi BM, et al. 2024. Genomic surveillance as a scalable framework for precision phage therapy against antibiotic-resistant pathogens. Cell 187:5901–5918. https://doi.org/10.1016/j.cell.2024.09.009

23. Wheatley RM, MacLean RC. 2021. CRISPR-Cas systems restrict horizontal gene transfer in *Pseudomonas aeruginosa*. ISME J 15:1420–1433. https://doi.org/10.1038/s41396-020-00860-3

24. Yadav G, Singh R. 2022. *In silico* analysis reveals the co-existence of CRISPR-Cas type I-F1 and type I-F2 systems and its association with restricted phage invasion in *Acinetobacter baumannii*. Front Microbiol 13:909886. https://doi.org/10.3389/fmicb.2022.909886

25. He F. 2011. *E. coli* genomic DNA extraction. Bio Protoc 1. https://doi.org/10.21769/BioProtoc.97

26. Prjibelski A, Antipov D, Meleshko D, Lapidus A, Korobeynikov A. 2020. Using SPAdes de novo assembler. Curr Protoc Bioinformatics 70:e102. https://doi.org/10.1002/cpbi.102

27. Boisvert S, Laviolette F, Corbeil J. 2010. Ray: simultaneous assembly of reads from a mix of high-throughput sequencing technologies. J Comput Biol 17:1519–1533. https://doi.org/10.1089/cmb.2009.0238

28. Chklovski A, Parks DH, Woodcroft BJ, Tyson GW. 2023. CheckM2: a rapid, scalable and accurate tool for assessing microbial genome quality using machine learning. Nat Methods 20:1203–1212. https://doi.org/10.1038/s41592-023-01940-w

29. Higgins PG, Prior K, Harmsen D, Seifert H. 2017. Development and evaluation of a core genome multilocus typing scheme for whole-genome sequence-based typing of *Acinetobacter baumannii*. PLoS One 12:e0179228. https://doi.org/10.1371/journal.pone.0179228

30. Silva M, Machado MP, Silva DN, Rossi M, Moran-Gilad J, Santos S, Ramirez M, Carriço JA. 2018. chewBBACA: A complete suite for gene-by-gene schema creation and strain identification. Microb Genom 4:e000166. https://doi.org/10.1099/mgen.0.000166

31. Mixão V, Pinto M, Sobral D, Di Pasquale A, Gomes JP, Borges V. 2023. ReporTree: a surveillance-oriented tool to strengthen the linkage between pathogen genetic clusters and epidemiological data. Genome Med 15:43. https://doi.org/10.1186/s13073-023-01196-1

32. Zhou Z, Alikhan NF, Sergeant MJ, Luhmann N, Vaz C, Francisco AP, Carriço JA, Achtman M. 2018. GrapeTree: visualization of core genomic relationships among 100,000 bacterial pathogens. Genome Res 28:1395–1404. https://doi.org/10.1101/gr.232397.117

33. Minh BQ, Schmidt HA, Chernomor O, Schrempf D, Woodhams MD, von Haeseler A, Lanfear R. 2020. IQ-TREE 2: new models and efficient methods for phylogenetic inference in the genomic era. Mol Biol Evol 37:1530–1534. https://doi.org/10.1093/molbev/msaa015

34. Kalyaanamoorthy S, Minh BQ, Wong TKF, von Haeseler A, Jermiin LS. 2017. ModelFinder: fast model selection for accurate phylogenetic estimates. Nat Methods 14:587–589. https://doi.org/10.1038/nmeth.4285

35. Hoang DT, Chernomor O, Haeseler A, Minh BQ, Vinh LS. 2018. UFBoot2: improving the ultrafast bootstrap approximation. Mol. Biol. Evol 35:518–522. https://doi.org/10.5281/zenodo.854445

36. Letunic I, Bork P. 2024. Interactive Tree of Life (iTOL) v6: recent updates to the phylogenetic tree display and annotation tool. Nucleic Acids Res 52:W78–W82. https://doi.org/10.1093/nar/gkae268

37. Jolley KA, Bray JE, Maiden MCJ. 2018. Open-access bacterial population genomics: BIGSdb software, the PubMLST.org website and their applications. Wellcome Open Res 3:124. https://doi.org/10.12688/wellcomeopenres.14826.1

38. Diancourt L, Passet V, Nemec A, Dijkshoorn L, Brisse S. 2010. The population structure of *Acinetobacter baumannii*: expanding multiresistant clones from an ancestral susceptible genetic pool. PLoS One 5:e10034. https://doi.org/10.1371/journal.pone.0010034

39. 2021. *Performance Standards for Antimicrobial Susceptibility Testing*. 31st ed. Clinical and Laboratory Standards Institute.

40. Bortolaia V, Kaas RS, Ruppe E, Roberts MC, Schwarz S, Cattoir V, Philippon A, Allesoe RL, Rebelo AR, Florensa AF, et al. 2020. ResFinder 4.0 for predictions of phenotypes from genotypes. J Antimicrob Chemother 75:3491–3500. https://doi.org/10.1093/jac/dkaa345

41. Fortier LC, Moineau S. 2007. Morphological and genetic diversity of temperate phages in *Clostridium difficile*. Appl Environ Microbiol 73:7358–7366. https://doi.org/10.1128/AEM.00582-07

42. Kutter E. 2009. Phage host range and efficiency of plating BT, p 141–149. In Bacteriophages: methods and protocols, volume 1: isolation, characterization, and interactions. Humana Press, Totowa, NJ.

43. Payne LJ, Todeschini TC, Wu Y, Perry BJ, Ronson CW, Fineran PC, Nobrega FL, Jackson SA. 2021. Identification and classification of antiviral defence systems in bacteria and archaea with PADLOC reveals new system types. Nucleic Acids Res 49:10868–10878. https://doi.org/10.1093/nar/gkab883

44. Couvin D, Bernheim A, Toffano-Nioche C, Touchon M, Michalik J, Néron B, Rocha EPC, Vergnaud G, Gautheret D, Pourcel C. 2018. CRISPRCas-Finder, an update of CRISRFinder, includes a portable version, enhanced performance and integrates search for Cas proteins. Nucleic Acids Res 46:W246–W251. https://doi.org/10.1093/nar/gky425

45. Grissa I, Vergnaud G, Pourcel C. 2007. CRISPRFinder: a web tool to identify clustered regularly interspaced short palindromic repeats. Nucleic Acids Res 35:W52–7. https://doi.org/10.1093/nar/gkm360

46. Biswas A, Staals RHJ, Morales SE, Fineran PC, Brown CM. 2016. CRISPRDetect: a flexible algorithm to define CRISPR arrays. BMC Genomics 17:356. https://doi.org/10.1186/s12864-016-2627-0

47. Dion MB, Labrie SJ, Shah SA, Moineau S. 2018. CRISPRStudio: a user-friendly software for rapid CRISPR array visualization. Viruses 10:602. https://doi.org/10.3390/v10110602

48. Camacho C, Coulouris G, Avagyan V, Ma N, Papadopoulos J, Bealer K, Madden TL. 2009. BLAST+: architecture and applications. BMC Bioinformatics 10:421. https://doi.org/10.1186/1471-2105-10-421

49. Schmartz GP, Hartung A, Hirsch P, Kern F, Fehlmann T, Müller R, Keller A. 2022. PLSDB: advancing a comprehensive database of bacterial plasmids. Nucleic Acids Res 50:D273–D278. https://doi.org/10.1093/nar/gkab1111

50. Galata V, Fehlmann T, Backes C, Keller A. 2019. PLSDB: a resource of complete bacterial plasmids. Nucleic Acids Res 47:D195–D202. https://doi.org/10.1093/nar/gky1050

51. Turton JF, Woodford N, Glover J, Yarde S, Kaufmann ME, Pitt TL. 2006. Identification of *Acinetobacter baumannii* by detection of the blaOXA-51-like carbapenemase gene intrinsic to this species. J Clin Microbiol 44:2974–2976. https://doi.org/10.1128/JCM.01021-06

52. Rodriguez-R LM, Conrad RE, Viver T, Feistel DJ, Lindner BG, Venter SN, Orellana LH, Amann R, Rossello-Mora R, Konstantinidis KT. 2024. An ANI gap within bacterial species that advances the definitions of intra-species units. MBio 15:e0269623. https://doi.org/10.1128/mbio.02696-23

53. Gaiarsa S, Batisti Biffignandi G, Esposito EP, Castelli M, Jolley KA, Brisse S, Sassera D, Zarrilli R. 2019. Comparative analysis of the two *Acinetobacter baumannii* multilocus sequence typing (MLST) schemes. Front Microbiol 10:930. https://doi.org/10.3389/fmicb.2019.00930

54. Shelenkov A, Akimkin V, Mikhaylova Y. 2023. International clones of high risk of *Acinetobacter baumannii*-definitions, history, properties and perspectives. Microorganisms 11:2115. https://doi.org/10.3390/microorganisms11082115

55. Rodrigues DLN, Morais-Rodrigues F, Hurtado R, Dos Santos RG, Costa DC, Barh D, Ghosh P, Alzahrani KJ, Soares SC, Ramos R, Góes-Neto A, Azevedo V, Aburjaile FF. 2021. Pan-resistome insights into the multidrug resistance of *Acinetobacter baumannii* Antibiotics (Basel) 10:596. https://doi.org/10.3390/antibiotics10050596

56. Chagas TPG, Carvalho KR, de Oliveira Santos IC, Carvalho-Assef APD, Asensi MD. 2014. Characterization of carbapenem-resistant *Acinetobacter baumannii* in Brazil (2008-2011): countrywide spread of OXA-23-producing clones (CC15 and CC79). Diagn Microbiol Infect Dis 79:468–472. https://doi.org/10.1016/j.diagmicrobio.2014.03.006

57. Camargo CH, Cunha MPV, de Barcellos TAF, Bueno MS, Bertani AM de J, Dos Santos CA, Nagamori FO, Takagi EH, Chimara E, de Carvalho E, Tiba-Casas MR. 2020. Genomic and phenotypic characterisation of antimicrobial resistance in carbapenem-resistant *Acinetobacter baumannii* hyperendemic clones CC1, CC15, CC79 and CC25. Int J Antimicrob Agents 56:106195. https://doi.org/10.1016/j.ijantimicag.2020.106195

58. Migliaccio A, Bray J, Intoccia M, Stabile M, Scala G, Jolley KA, Brisse S, Zarrilli R. 2023. Phylogenomics of *Acinetobacter* species and analysis of antimicrobial resistance genes. Front Microbiol 14:1264030. https://doi.org/10.3389/fmicb.2023.1264030

59. Falagas ME, Vardakas KZ, Roussos NS. 2015. Trimethoprim/sulfamethoxazole for *Acinetobacter* spp.: a review of current microbiological and clinical evidence. Int J Antimicrob Agents 46:231–241. https://doi.org/10.1016/j.ijantimicag.2015.04.002

60. Lashinsky JN, Henig O, Pogue JM, Kaye KS. 2017. Minocycline for the treatment of multidrug and extensively drug-resistant *A. baumannii*: a review. Infect Dis Ther 6:199–211. https://doi.org/10.1007/s40121-017-0153-2

61. Chuang YC, Cheng A, Sun HY, Wang JT, Chen YC, Sheng WH, Chang SC. 2019. Microbiological and clinical characteristics of *Acinetobacter baumannii* bacteremia: implications of sequence type for prognosis. J Infect 78:106–112. https://doi.org/10.1016/j.jinf.2018.10.001

62. Liu M, Hernandez-Morales A, Clark J, Le T, Biswas B, Bishop-Lilly KA, Henry M, Quinones J, Voegtly LJ, Cer RZ, Hamilton T, Schooley RT, Salka S, Young R, Gill JJ. 2022. Comparative genomics of *Acinetobacter baumannii* and therapeutic bacteriophages from a patient undergoing phage therapy. Nat Commun 13:3776. https://doi.org/10.1038/s41467-022-31455-5

63. Gordillo Altamirano F, Forsyth JH, Patwa R, Kostoulias X, Trim M, Subedi D, Archer SK, Morris FC, Oliveira C, Kielty L, Korneev D, O'Bryan MK, Lithgow TJ, Peleg AY, Barr JJ. 2021. Bacteriophage-resistant *Acinetobacter baumannii* are resensitized to antimicrobials. Nat Microbiol 6:157–161. https://doi.org/10.1038/s41564-020-00830-7

64. Bai J, Raustad N, Denoncourt J, van Opijnen T, Geisinger E. 2023. Genome-wide phage susceptibility analysis in Acinetobacter baumannii reveals capsule modulation strategies that determine phage infectivity. PLoS Pathog 19:e1010928. https://doi.org/10.1371/journal.ppat.1010928

65. Bernheim A, Sorek R. 2020. The pan-immune system of bacteria: antiviral defence as a community resource. Nat Rev Microbiol 18:113–119. https://doi.org/10.1038/s41579-019-0278-2

66. Vassallo CN, Doering CR, Littlehale ML, Teodoro GIC, Laub MT. 2022. A functional selection reveals previously undetected anti-phage defence systems in the *E. coli* pangenome. Nat Microbiol 7:1568–1579. https://doi.org/10.1038/s41564-022-01219-4

67. Millman A, Melamed S, Amitai G, Sorek R. 2020. Diversity and classification of cyclic-oligonucleotide-based anti-phage signalling systems. Nat Microbiol 5:1608–1615. https://doi.org/10.1038/s41564-020-0777-y

68. Makarova KS, Wolf YI, Iranzo J, Shmakov SA, Alkhnbashi OS, Brouns SJJ, Charpentier E, Cheng D, Haft DH, Horvath P, et al. 2020. Evolutionary classification of CRISPR-Cas systems: a burst of class 2 and derived variants. Nat Rev Microbiol 18:67–83. https://doi.org/10.1038/s41579-019-0299-x

69. Tyumentseva M, Mikhaylova Y, Prelovskaya A, Tyumentsev A, Petrova L, Fomina V, Zamyatin M, Shelenkov A, Akimkin V. 2021. Genomic and phenotypic analysis of multidrug-resistant *Acinetobacter baumannii* clinical isolates carrying different types of CRISPR/Cas systems. Pathogens 10:205. https://doi.org/10.3390/pathogens10020205

70. Amitai G, Sorek R. 2016. CRISPR-Cas adaptation: insights into the mechanism of action. Nat Rev Microbiol 14:67–76. https://doi.org/10.1038/nrmicro.2015.14

71. Pursey E, Dimitriu T, Paganelli FL, Westra ER, van Houte S. 2022. CRISPR-Cas is associated with fewer antibiotic resistance genes in bacterial pathogens. Phil Trans R Soc B 377:20200464. https://doi.org/10.1098/rstb.2020.0464

72. Martínez-Trejo A, Ruiz-Ruiz JM, Gonzalez-Avila LU, Saldaña-Padilla A, Hernández-Cortez C, de Jesús Colmenero-Solís R, Bello-López JM, Castro-Escarpulli G. 2024. The CRISPR-Cas system in clinical strains of Acinetobacter baumannii: an in-silico analysis. Lett Appl Microbiol 77:vae003. https://doi.org/10.1093/lambio/ovae003

73. Palmer KL, Gilmore MS. 2010. Multidrug-resistant enterococci lack CRISPR-cas. MBio 1:e00227-10. https://doi.org/10.1128/mBio.00227-10

74. Mangas EL, Rubio A, Álvarez-Marín R, Labrador-Herrera G, Pachón J, Pachón-Ibáñez ME, Divina F, Pérez-Pulido AJ. 2019. Pangenome of *Acinetobacter baumannii* uncovers two groups of genomes, one of them with genes involved in CRISPR/Cas defence systems associated with the absence of plasmids and exclusive genes for biofilm formation. Microb Genom 5. https://doi.org/10.1099/mgen.0.000309

75. Horvath P, Barrangou R. 2010. CRISPR/Cas, the immune system of bacteria and archaea. Science 327:167–170. https://doi.org/10.1126/science.1179555

76. Noel HR, Petrey JR, Palmer LD. 2022. Mobile genetic elements in *Acinetobacter* antibiotic-resistance acquisition and dissemination. Ann N Y Acad Sci 1518:166–182. https://doi.org/10.1111/nyas.14918

77. Jeon JH, Jang KM, Lee JH, Kang LW, Lee SH. 2023. Transmission of antibiotic resistance genes through mobile genetic elements in *Acinetobacter baumannii* and gene-transfer prevention. Sci Total Environ 857:159497. https://doi.org/10.1016/j.scitotenv.2022.159497

78. Shehreen S, Chyou T, Fineran PC, Brown CM. 2019. Genome-wide correlation analysis suggests different roles of CRISPR-Cas systems in the acquisition of antibiotic resistance genes in diverse species. Phil Trans R Soc B 374:20180384. https://doi.org/10.1098/rstb.2018.0384

79. Wang Y, Yang J, Sun X, Li M, Zhang P, Zhu Z, Jiao H, Guo T, Li G. 2022. CRISPR-Cas in *Acinetobacter baumannii* contributes to antibiotic susceptibility by targeting endogenous *AbaI*. Microbiol Spectr 10:e0082922. https://doi.org/10.1128/spectrum.00829-22

80. Dion MB, Shah SA, Deng L, Thorsen J, Stokholm J, Krogfelt KA, Schjørring S, Horvath P, Allard A, Nielsen DS, Petit M-A, Moineau S. 2024. *Escherichia coli* CRISPR arrays from early life fecal samples preferentially target prophages. ISME J 18:wrae005. https://doi.org/10.1093/ismejo/wrae005

81. Song S, Semenova E, Severinov K, Fernández-García L, Benedik MJ, Maeda T, Wood TK. 2022. CRISPR-cas controls cryptic prophages. Int J Mol Sci 23:16195. https://doi.org/10.3390/ijms232416195